Nonstationary neutron diffraction by surface acoustic waves

G. V. Kulin,[1] A. I. Frank,[1] V. A. Bushuev,[2] Yu. N. Khaydukov,[2,3,4] D. V. Roshchupkin,[5] S. Vadilonga,[6] and A. P. Sergeev[7]

[1]*Joint Institute for Nuclear Research, 141980 Dubna, Russia*
[2]*Moscow State University, 119991 Moscow, Russia*
[3]*Max-Planck-Institut für Festkörperforschung, Heisenbergstraße 1, D-70569 Stuttgart, Germany*
[4]*Max Planck Society Outstation at the Heinz Maier-Leibnitz Zentrum (MLZ), D-85748 Garching, Germany*
[5]*Institute of Microelectronics Technology and High-Purity Materials Russian Academy of Sciences, 142432 Chernogolovka, Moscow District, Russia*
[6]*Institute for Nanometre Optics and Technology, Helmholtz-Zentrum Berlin für Materialien und Energie, 14109 Berlin, Germany*
[7]*Federal State Institution Scientific Research Institute for System Analysis of the Russian Academy of Sciences, 117218 Moscow, Russia*

(Received 27 December 2019; revised manuscript received 13 March 2020; accepted 16 March 2020; published 20 April 2020)

Theory of neutron diffraction on traveling and standing surface acoustic waves (SAWs) is considered. Results of experiment on observation of neutron diffraction by a SAW traveling both along and against the direction of a neutron wave, as well as a standing SAW, are presented. The experimental results are mostly consistent with theoretical predictions.

DOI: 10.1103/PhysRevB.101.165419

I. INTRODUCTION

Unlike conventional acousto-optics, the history of which dates back almost 90 years [1–5], x-ray [6–9] and neutron [10–14] acousto-optics arose half a century later. In neutron experiments, similar to x-ray experiments, Bragg diffraction on an ultrasound (US) excited crystal was initially investigated. Later these experiments were complemented by studies of influence of acoustic waves excited on the surface of a crystal on Bragg diffraction of neutrons [15–17].

As for neutron diffraction on a surface wave itself, the possibility of existence of this phenomenon was first discussed in Ref. [18] as a possible reason for inelastic neutron scattering, which leads to a decrease in the storage time of ultracold neutrons (UCNs) in traps. The first—and until recently, only—experiment [19] on the observation of neutron diffraction by traveling surface acoustic wave (SAW) was carried out much later. In Ref. [20], neutron diffraction on acoustic wave traveling on the surface of a thin film was considered as a possible method for studying the properties of such films. Theoretical consideration of inelastic scattering of UCNs by waves traveling along the surface of a liquid has been the subject of papers [21,22].

Unlike electromagnetic waves with velocities of many orders of magnitude higher than the velocity of a SAW, velocity of thermal and cold neutrons is usually several times lower than the velocity of a SAW. In the case of the slowest UCNs, difference in the velocities of US and neutron waves is already several orders of magnitude. In this sense, physics of neutron diffraction on US is very similar to the repeatedly observed phenomenon of neutron diffraction on moving gratings [23–25].

This work is devoted to the theoretical and experimental study of neutron diffraction by SAW. A new appeal to this problem is related to several circumstances. First, during the time since the experiment [19], a significant progress in neutron technique was achieved, thus allowing us to study the phenomenon with better accuracy and in wide ranges of neutron wavelengths and ultrasonic wave frequencies.

The second important circumstance is the desire to expand the range of the studied phenomena and, in addition to diffraction by traveling SAWs, also observe diffraction on standing waves. In the latter case, we deal with a nonstationary quantum phenomenon of reflection from an oscillating potential, very close to the previously observed reflection of neutrons from a vibrating mirror [26].

It is known that in the SAW diffraction, the amplitude of the first diffraction order essentially depends on the value of the normal component of the wave vector in the substance on the surface of which the wave runs [19]. This amplitude is determined by Fresnel formulas and the dispersion law of neutrons in the substance. However, when a Rayleigh wave is excited on the surface of the substrate, a sufficiently thick layer of matter is involved in the vibrational motion, the thickness of which is of the order of the SAW wavelength. For the typical values of frequency and amplitude of the ultrasonic wave, the atoms in this layer move with alternating acceleration with a magnitude reaching values of the order of 10^8 m/s^2. Therefore, measurement of the amplitudes of diffraction orders can provide information on the dispersion law of neutron waves in matter moving with giant acceleration [27,28].

II. NEUTRON DIFFRACTION BY SURFACE WAVES. THEORY

Everywhere below, we will talk about diffraction of cold neutrons with a wavelength of several angstroms on surface

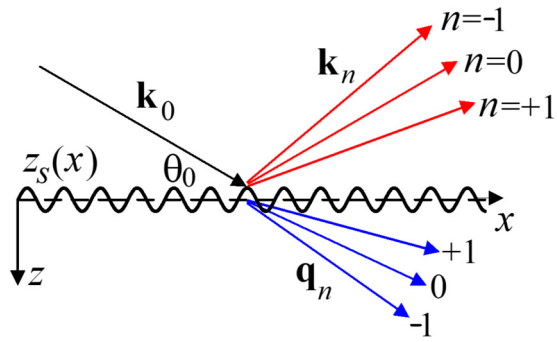

FIG. 1. Sketch of a neutron diffraction on a stationary harmonic grating.

waves generated on the surface of a substance. It is assumed that neutrons incident on the surface of the medium at a sufficiently small angle θ, so the intensity of the reflected waves can be measured. The smallness of the angle and a certain orientation of the surface relative to the crystallographic axes of the sample makes it impossible to fulfill the Bragg condition, which allows one to completely ignore the internal structure of the substance and consider the medium as homogeneous. It is known that the dispersion law of neutron waves in matter with good accuracy satisfies the equation

$$k^2 = k_0^2 - 4\pi\rho b, \tag{1}$$

where k and k_0 are wave numbers in medium and vacuum, respectively, ρ is the number of nuclei per unit volume, and b is the average bound coherent scattering (see Ref. [29]). In the case of $b = \text{const}$, a similar relation takes place for the components of wave vectors normal to the surface of the medium $k_\perp$ and $k_{0\perp}$ [30]. When $k_{0\perp} = k_0 \sin\theta \leqslant \sqrt{4\pi\rho b}$, a total external reflection takes place.

In previous works devoted to neutron diffraction on a traveling wave [18,19] or on a moving grating [23–25], the study was conducted in the rest system of the structure with the subsequent transformation of the resulting wave function into a laboratory coordinate system. As it will be shown below, it is not necessary at all to resort to a transition to a moving coordinate system to find a solution of the problem of nonstationary diffraction on a traveling or standing wave.

From a methodological point of view, it seems useful to start by solving a stationary problem in which the surface of a substance has a sinusoidal shape. In the next two sections, we will move on to the case of traveling and standing acoustic waves.

A. Diffraction on a surface with harmonic profile

Let us consider a homogeneous medium characterized by a certain scattering length density ρb, which corresponds to the critical wave number $k_b = \sqrt{4\pi\rho b}$. The surface profile of the medium is defined by a periodic harmonic function:

$$z_S(x) = a\sin(Qx). \tag{2}$$

The x axis is directed along the averaged surface and the z axis is directed normal to it into the interior of the medium (Fig. 1). The sinusoidal shape of the surface Eq. (2) forms a harmonic diffraction grating with a spatial period Λ along the x axis, with $Q = 2\pi/\Lambda$ being the minimum modulus of the reciprocal lattice vector.

A plain monochromatic neutron wave $\Psi_0(x, z, t)$ with wave vector $\mathbf{k_0}$, projections $k_{0x} = k_0\cos\theta_0$, $k_{0z} = k_0\sin\theta_0$, and energy $E_0 = \hbar\omega_0 = \hbar^2 k_0^2/2M$, where M is the neutron mass, is incident on the vacuum-medium interface at an angle θ_0 to the average surface:

$$\Psi_0(x, z, t) = \exp(ik_{0x}x + ik_{0z}z - i\omega_0 t). \tag{3}$$

As a result of diffraction on the grating, a set of diffracted plane waves with wave vectors $\mathbf{k_n}$ and amplitudes r_n is formed in the upper half-space ($z \leqslant z_S$). Here $n = 0, \pm1, \pm2, ..$ are the numbers of diffraction orders. Similarly, a set of transmitted (diffracted) waves with wave vectors $\mathbf{q_n}$ and amplitudes t_n (Fig. 1) is formed in the lower half-space ($z > z_S$). The reflected and transmitted wave functions can be written as

$$\Psi_R(x, z, t) = \sum_{n=-\infty}^{\infty} r_n \exp(ik_{nx}x - ik_{nz}z - i\omega_0 t), \tag{4a}$$

$$\Psi_T(x, z, t) = \sum_{n=-\infty}^{\infty} t_n \exp(iq_{nx}x + iq_{nz}z - i\omega_0 t), \tag{4b}$$

where

$$k_{nz} = \left(k_0^2 - k_{nx}^2\right)^{1/2}, \quad q_{nz} = \left(k_{nz}^2 - k_b^2\right)^{1/2}. \tag{5}$$

In relations Eq. (5), the continuity condition for the tangential components of the wave vectors $q_{nx} = k_{nx}$ is used. The unknown quantities to be found are r_n, k_{nx}, k_{nz}, and t_n, q_{nz}. They can be obtained from the continuity conditions of wave functions and their normal derivatives on the surface $z = z_S(x)$:

$$\Psi_0(x, z_S, t) + \Psi_R(x, z_S, t) = \Psi_T(x, z_S, t), \tag{6a}$$

$$\frac{d}{dz}\Psi_0(x, z, t)_{z=z_S} + \frac{d}{dz}\Psi_R(x, z, t)_{z=z_S} = \frac{d}{dz}\Psi_T(x, z, t)_{z=z_S}. \tag{6b}$$

Formula Eq. (6b) is approximate. It is more correct to write it taking into account the calculation of the derivative normal to the surface at each local point (x, z_S), which does not coincide exactly with the normal derivative to the "average" surface, i.e., along the z axis (see Ref. [31] for more details). However, such an approximation is justified if the grating is fairly smooth, i.e., the depth of its profile is much less than the period: $a \ll \Lambda$. In the experiments described below, $a \sim$ 10–20 Å, and $\Lambda \approx 50\ \mu$m.

Due to the stationarity of the problem, all waves have the same frequency ω_0, so in the further calculations of this section we will omit the term $i\omega_0 t$ in exponents Eqs. (3) and (4), being interested only in the coordinate parts of the wave functions. The wave function of incident neutrons Eq. (3) on the surface of a medium with a sinusoidal profile Eq. (2) has the form

$$\Psi_0(x, z_S) = \exp(ik_{0x}x) \times \exp[ik_{0z}a\sin(Qx)]. \tag{7}$$

Let us use a well-known relation to decompose the exponent of a special kind over Bessel functions of the first

kind:

$$\exp(i\beta\sin\varphi) = \sum_{m=-\infty}^{\infty} J_m(\beta)\exp(im\varphi). \tag{8}$$

Then

$$\Psi_0(x, z_S) = \sum_{m=-\infty}^{\infty} J_m(k_{0z}a)\exp[i(k_{0x}+mQ)x]. \tag{9}$$

Thus, a plane monochromatic wave Eq. (3) incident on a periodically deformed surface is represented by the sum of plane waves Eq. (9) with amplitudes J_m and x projections of wave vectors $k_{mx} = k_{0x} + mQ$. Similarly, the wave functions of diffracted waves Eqs. (4) in the upper half-space and in the medium can be represented as

$$\Psi_R(x, z_S) = \sum_n \sum_{m'} r_n J_{m'}(-k_{nz}a)\exp[i(k_{nx}+m'Q)x], \tag{10a}$$

$$\Psi_T(x, z_S) = \sum_n \sum_{m'} t_n J_{m'}(q_{nz}a)\exp[i(k_{nx}+m'Q)x]. \tag{10b}$$

Inserting relations Eqs. (9) and (10) into Eq. (6a), we write the first continuity equation:

$$\begin{aligned}&\sum_{m=-\infty}^{\infty} J_m(k_{0z}a)\exp[i(k_{0x}+mQ)x]\\ &+\sum_n\sum_{m'} r_n J_{m'}(-k_{nz}a)\exp[i(k_{nx}+m'Q)x]\\ &=\sum_n\sum_{m'} t_n J_{m'}(q_{nz}a)\exp[i(k_{nx}+m'Q)x].\end{aligned} \tag{11}$$

Let us take into account that the boundary condition Eq. (11) must be satisfied at any point x on the surface. Hence it follows that $k_{0x} + mQ = k_{nx} + m'Q$ or $k_{nx} = k_{0x} + (m - m')Q$. Since the difference of integers is also an integer, by introducing the notation $n = m - m'$ and replacing the summation index $m' = m - n$ in Eq. (11), we obtain

$$k_{nx} = k_0\cos\theta_n = k_{0x} + nQ, \tag{12}$$

where n and θ_n are diffraction order and angle, correspondingly. In what follows, we restrict ourselves to considering such quantities nQ in Eq. (12) so $|k_{nx}| < k_0$, and, hence, $\mathrm{Im}(k_{nz}) = 0$. Reducing exponentials in Eq. (11) with the same exponents, we obtain the relation

$$J_m(k_{0z}a) + \sum_n r_n J_{m-n}(-k_{nz}a) = \sum_n t_n J_{m-n}(q_{nz}a). \tag{13a}$$

Similarly, from Eqs. (6b), (9), and (10), it follows that

$$k_{0z}J_m(k_{0z}a) - \sum_n r_n k_{nz} J_{m-n}(-k_{nz}a) = \sum_n t_n q_{nz} J_{m-n}(q_{nz}a). \tag{13b}$$

The system of equations Eqs. (13a) and (13b) determines a solution for the amplitudes of diffraction orders r_n and t_n.

Significant simplification and simple analytical solutions are obtained in the case usually realized in experiment, small arguments $\xi \ll 1$ of Bessel function $J_n(\xi)$:

$$J_0(\xi) \approx 1, J_1(\pm\xi) \approx \pm\xi/2, J_{-1}(\pm\xi) \approx \mp\xi/2. \tag{14}$$

In this case, it is sufficient to confine ourselves to the terms with $n = 0, \pm1$ in Eq. (13) and consider the cases with $m = 0, \pm1$, neglecting members of higher orders of smallness $r_{\pm1}J_{\pm1}$, $t_{\pm1}J_{\pm1}$, $J_{\pm2}$, and so on.

(a) Case $m = 0$. Equations (13a) and (13b) in approximation Eq. (14) immediately lead to relations

$$1 + r_0 = t_0, \quad k_{0z}(1 - r_0) = q_{0z}t_0, \tag{15}$$

from which, for zero-order amplitudes, we obtain the well-known Fresnel formulas for the reflection and refraction of waves from a flat surface:

$$r_0 = \frac{k_{0z} - q_{0z}}{k_{0z} + q_{0z}}, \quad t_0 = \frac{2k_{0z}}{k_{0z} + q_{0z}}, \tag{16}$$

where $q_{0z} = (k_{0z}^2 - k_b^2)^{1/2}$.

(b) Case $m = 1$. From Eq. (13a), it follows:

$$k_{0z}a(1 - r_0)/2 + r_1 = q_{0z}at_0/2 + t_1. \tag{17}$$

Taking into account the second expression in Eq. (15), one obtains $r_1 = t_1$.

Similarly, from the continuity condition for the derivatives Eq. (13b), taking into account expansion Eq. (14), we obtain

$$k_{0z}^2a(1 + r_0)/2 - k_{1z}r_1 = q_{0z}^2at_0/2 + q_{1z}t_1, \tag{18}$$

whence, after taking into account the relations $1 + r_0 = t_0$ Eq. (15) and $r_1 = t_1$, we arrive at the expression for the first-order diffraction reflection amplitude:

$$r_1 = k_{0z}a\frac{k_{0z} - q_{0z}}{k_{1z} + q_{1z}}, \tag{19}$$

where $k_{1z} = (k_{0z}^2 - 2k_{0x}Q)^{1/2}$, $q_{1z} = (k_{0z}^2 - 2k_{0x}Q - k_b^2)^{1/2}$. Hereinafter, we neglect the small quadratic terms $\sim Q^2$, which is justified for $Q \ll k_{0x}$.

(c) Case $m = -1$. Quite similarly to the previous calculations, we obtain for the amplitudes of diffraction waves of the minus first-order $r_{-1} = t_{-1}$, and

$$r_{-1} = -k_{0z}a\frac{k_{0z} - q_{0z}}{k_{-1z} + q_{-1z}}, \tag{20}$$

where $k_{-1z} = (k_{0z}^2 + 2k_{0x}Q)^{1/2}$, $q_{-1z} = (k_{0z}^2 + 2k_{0x}Q - k_b^2)^{1/2}$.

One should bear in mind that since the integral neutron flux depends on the ratio between the angles of the incident and diffracted waves, the intensity of the corresponding waves, proportional to the flux density, is not equal to the square of the wave amplitude modulus. Therefore, the reflection and transmission coefficients have the form

$$R_n = \frac{k_{nz}}{k_{0z}}|r_n|^2, \quad T_n = \frac{\mathrm{Re}(q_{nz})}{k_{0z}}|t_n|^2. \tag{21}$$

It is also useful to determine angular distribution of diffracted waves. Taking into account the invariance of the total wave number, it is easy to obtain the following expressions for diffraction angles from relation Eq. (12) (see also Fig. 1):

$$\sin^2\theta_n = \sin^2\theta_0 - \frac{2k_{0x}nQ}{k_0^2} - \frac{n^2Q^2}{k_0^2}, \tag{22a}$$

$$\theta_n^2 \cong \theta_0^2 - 2nQ/k_0. \tag{22b}$$

B. Diffraction on a traveling surface acoustic wave

Having obtained in the previous Sec. II A the relations for neutron diffraction by a static wave, it is easy to modify these results for the case of a traveling SAW. The equation of the surface of the medium along which acoustic wave runs now has the following form:

$$z_S(x,t) = a\sin(sQx - \Omega t), \tag{23}$$

where $\Omega = 2\pi/T = 2\pi V/\Lambda$ is the frequency, $Q = 2\pi/\Lambda = \Omega/V$ is the wave vector length, V is the velocity, and Λ is the wavelength (spatial period) of the acoustic wave. The index s in Eq. (23) determines direction of the traveling wave: $s = +1$, if the wave runs in positive direction of the x axis, and $s = -1$ for the negative case.

Reflected and transmitted diffracted waves of different orders now possess different frequencies:

$$\Psi_R(x,z,t) = \sum_{n=-\infty}^{\infty} r_n \exp(ik_{nx}x - ik_{nz}z - i\omega_n t), \tag{24a}$$

$$\Psi_T(x,z,t) = \sum_{n=-\infty}^{\infty} t_n \exp(ik_{nx}x + iq_{nz}z - i\omega_n t). \tag{24b}$$

The time dependence of the wave functions appearing here requires taking it into account when writing the continuity Eqs. (6). Having written down the boundary condition for the incident wave on the surface of the medium, and using as above expansion Eq. (8), we obtain instead of Eq. (9)

$$\Psi_0(x,z_S,t) = \sum_{m=-\infty}^{\infty} J_m(k_{0z}a)\exp(ik_{mx}x - i\omega_m t), \tag{25}$$

where now $k_{mx} = k_{0x} + smQ$, $\omega_m = \omega_0 + m\Omega$.

Thus, on an oscillating interface with a traveling SAW, the incident plane wave takes the form of a sum of plane waves not only with different amplitudes J_m and x projections of wave vectors k_{mx}, but also with different frequencies ω_m. In addition, projections of wave vectors also depend on the parameter s, i.e., on the direction of the surface wave propagation.

The further solution is quite similar to that described in the previous section. Instead of expression Eq. (12), the relation obtained after replacing the summation index now has the form

$$k_{nx} = k_{0x} + s(m - m')Q = k_{0x} + snQ. \tag{26}$$

This should be supplemented with a similar expression for frequencies

$$\omega_n = \omega_0 + (m - m')\Omega = \omega_0 + n\Omega. \tag{27}$$

The continuity equations on the interface $z_S = z_S(x,t)$ have the same form as Eqs. (13), however, the z components of the wave vectors in this expression now have the other form. Let us consider this question in more detail.

From Eq. (27), we can obtain an explicit form for the squares of the modules of wave vectors of different orders. Indeed, the total energy of neutrons is $\hbar\omega_n = \hbar^2 k_n^2/2M$. From here, after simple transformations, we get

$$k_n^2 = \frac{2M}{\hbar^2}[\hbar(\omega_0 + n\Omega)] = k_0^2 + 2nQk_V, \tag{28}$$

where $k_V = MV/\hbar$, which is formally equal to the magnitude of the wave vector of a neutron moving with a speed of V. Knowing the values of the squared wave vectors of diffracted waves in the upper hemisphere Eq. (28) and their x-projections Eq. (26), it is easy to obtain expressions for their z projections:

$$k_{nz}^2 = k_n^2 - k_{nx}^2 = k_{0z}^2 + 2nQ(k_V - sk_{0x}) - n^2Q^2. \tag{29}$$

The squared modules of the wave vectors in the medium differ from vacuum values on $k_b^2 = 4\pi\rho b$, hence

$$q_{nz}^2 = k_{0z}^2 + 2nQ(k_V - sk_{0x}) - n^2Q^2 - k_b^2. \tag{30}$$

Having thus determined the values of the z projections of the wave vectors, we can now calculate the amplitudes r_n, t_n, reflectivities R_n, and transmittances T_n Eqs. (21) of the diffracted waves. In the case of small SAW amplitudes, when expansions Eq. (14) are valid, we obtain for the amplitudes of waves of $n = 0, \pm 1$ diffraction orders the same relations Eqs. (16), (19), and (20) as in the case of a stationary grating, corrected, however, with new expressions for k_{nz} Eq. (29) and q_{nz} Eq. (30). Reflectivities for the first three orders, which were experimentally measured in the present paper (see Sec. III), have the following form:

$$R_0 = \left|\frac{k_{0z} - q_{0z}}{k_{0z} + q_{0z}}\right|^2, \quad R_{\pm 1} = k_{0z}k_{\pm 1z}a^2\left|\frac{k_{0z} - q_{0z}}{k_{\pm 1z} + q_{\pm 1z}}\right|^2. \tag{31}$$

Equations (31) coincide with expressions Eqs. (11a) and (11b) of Ref. [19].

Knowing the squares of the modules of wave vectors Eq. (28) and their z-projections $k_{nz} = k_n\sin\theta_n$ Eq. (29), it is easy to find diffraction angles θ_n. Given the smallness of the wave vector Q and all diffraction angles, we obtain

$$\theta_n^2 \approx \theta_0^2 + 2\frac{nQ}{k_0}\left(\frac{k_V}{k_0} - s\right). \tag{32}$$

A comparison of relations Eqs. (32) and (22) shows that if, for the case of ordinary diffraction, the angle $\theta_n < \theta_0$ for $n > 0$, then for the diffraction on a moving structure, the sign of the deviation of the diffraction order from a specular reflected zero-order wave depends also on the sign of the expression $[(k_V/k_0) - s]$.

In experiments on the diffraction of thermal neutrons on a traveling surface wave $k_V > k_0$, the sign of deviation of the n-order wave from the specular one is opposite to what takes place in conventional diffraction at both possible values of the parameter s.

C. Diffraction on a standing surface acoustic wave

The surface profile of the medium excited by a standing SAW can be defined as follows:

$$\begin{aligned} z_S(x,t) &= a_1\sin(Qx - \Omega t) + a_2\sin(-Qx - \Omega t) \\ &\equiv a_1\sin(Qx - \Omega t) - a_2\sin(Qx + \Omega t), \end{aligned} \tag{33}$$

where $a_{1,2}$ are the amplitudes of counterdirected surface waves with wave vectors $\pm Q$ and frequency Ω.

Let us consider the boundary condition for a plane monochromatic wave Eq. (3) incident on the vacuum/medium interface excited by a standing SAW. On the interface $z = z_S$,

the wave function Eq. (3) will take the following explicit form:

$$\Psi_0(x, z_S, t) = \exp(ik_{0x}x - i\omega_0 t) \times \exp[ik_{0z}a_1 \sin(Qx - \Omega t)] \times \exp[-ik_{0z}a_2 \sin(Qx + \Omega t)]. \quad (34)$$

Using, as above, the expansion Eq. (8) of the $\exp(i\beta \sin\varphi)$-type exponent in a series in Bessel functions, we write relation Eq. (34) as follows:

$$\Psi_0(x, z_S, t) = \exp(ik_{0x}x - i\omega_0 t) \times \left(\sum_{m=-\infty}^{\infty} J_m(k_{0z}a_1)\exp[im(Qx - \Omega t)]\right) \times \left(\sum_{m'=-\infty}^{\infty} J_{m'}(-k_{0z}a_2)\exp[im'(Qx + \Omega t)]\right). \quad (35)$$

Expression for the derivative $\partial\Psi_0(x, z, t)/\partial z|_{z=z_S}$ on the interface differs from formula Eq. (35) only by a factor ik_{0z}.

In contrast to the case of traveling SAW Eq. (25), where one sum appeared over the Bessel functions, in Eq. (35) there is a product of the sums, i.e., double sum over m and m', and subsequent calculations become more cumbersome. Therefore, we will initially proceed from assumption that the arguments of the Bessel functions $k_{mz}a_{1,2} \ll 1$ and $q_{mz}a_{1,2} \ll 1$ are small both in Eq. (35) and in the expressions for wave functions $\Psi_{R,T}(x, z_S, t)$. In addition, we restrict ourselves to the analysis of only zero and plus/minus first orders, i.e., $m, m' = 0, \pm 1$. From Eq. (35), it follows that the function $\Psi_0(x, z_S, t)$ has, in this case, a form of nine terms, of which only five have a nonvanishing order of smallness:

$$\Psi_0(x, z_S, t) = J_0(k_{0z}a_1)J_0(-k_{0z}a_2)\exp(ik_{0x}x - i\omega_0 t) + J_{-1}(k_{0z}a_1)J_0(-k_{0z}a_2)\exp[i(k_{0x} - Q)x - i(\omega_0 - \Omega)t] + J_0(k_{0z}a_1)J_{-1}(-k_{0z}a_2)\exp[i(k_{0x} - Q)x - i(\omega_0 + \Omega)t] + J_0(k_{0z}a_1)J_1(-k_{0z}a_2)\exp[i(k_{0x} + Q)x - i(\omega_0 - \Omega)t] + J_1(k_{0z}a_1)J_0(-k_{0z}a_2)\exp[i(k_{0x} + Q)x - i(\omega_0 + \Omega)t]. \quad (36)$$

Thus, the incident and diffracted waves at the interface are superpositions of five plane waves with the following projections of wave vectors and frequencies:

$$k_{nx} = k_{0x} + nQ, \quad (37a)$$

$$\omega_m = \omega_0 + mQ, \quad (37b)$$

where $n, m = 0, \pm 1$. There are certain restrictions on the possible values of the indices n and m. So, for the specular reflection ($n = 0$) the frequency index m in Eq. (37b) can not be equal to $+1$ or -1. For elastic scattering ($m = 0$), the index n in the x projection of the wave vector Eq. (37a) in the frame of this first-order approximation of smallness cannot be equal to $+1$ or -1.

Having set one of the amplitudes a_1 or a_2 in Eq. (36) to zero, it is easy to show that we automatically come to the case of the considered above traveling SAW Eq. (25) with either $s = +1$ (for $a_2 = 0$) or $s = -1$ (for $a_1 = 0$). In the case of standing wave Eq. (36), compared to, e.g., traveling to the right wave ($s = +1$), is characterized by the appearance of two new waves with exponents $\exp(ik_{1x}x - i\omega_{-1}t)$ and $\exp(ik_{-1x}x - i\omega_1 t)$.

It is obvious that the diffracted waves are characterized, as before, by a discrete spectrum of frequencies $\omega_m = \omega_0 + m\Omega$ that determine the magnitude of the wave vectors of corresponding waves. For the reflected waves, they are defined by obvious relation $k_m^2 = (2M/\hbar)\omega_m$ Eq. (28). The wave number (wave vector length) depends only on one index m. If we restrict ourself to $m = 0, \pm 1$ orders, there are three such wave numbers. At the same time, the x projections of the wave vectors of the diffracted waves are determined by the relation Eq. (37a) and they depend on the index n. Therefore, from what has been said above about the expansion of the incident wave, it follows that there will be five z projections of the wave vectors, and hence the diffraction angles. Qualitatively, this is easy to understand from Eq. (29), which determines the z-projections k_{nz} of the waves diffracted on a traveling wave. In addition to the diffraction order n, it also depends on a parameter s that determines the direction of the SAW propagation. In the considered case, a standing acoustic wave Eq. (33) is a superposition of two counterpropagating waves. Hence, for the description of the z projections of the wave vectors of diffracted waves above and below the interface, we will use in the following expressions, depending on the indices n and m,

$$k_{nz} \equiv k_{n,m} = \left(k_m^2 - k_{nx}^2\right)^{1/2} = \left[k_{0z}^2 + 2Q(mk_V - nk_{0x})\right]^{1/2}, \quad (38a)$$

$$q_{nz} \equiv q_{n,m} = \left(k_{n,m}^2 - k_b^2\right)^{1/2}, \quad (38b)$$

where we neglected the small quadratic terms n^2Q^2. Here, a combination of indices (n, m) are the following: (0,0), $(-1, -1)$, $(-1,+1)$, $(+1,-1)$, (1,1). It is easy to see that for the specular reflection, $k_{0,0} \equiv k_{0z}$ and $q_{0,0} \equiv q_{0z}$.

Knowledge of the magnitudes of wave vectors in vacuum $k_m = k_0 + mk_V Q/k_0$ [see Eq. (28)] and corresponding x-projections k_{nx} Eq. (37a) allows for determination of the diffraction angles from the expression

$$k_m \cos\theta_{n,m} = k_0 \cos\theta_0 + nQ. \quad (39)$$

From this, for small diffraction angles, it is easy to obtain following expression for squares of diffraction angles:

$$\theta_{n,m}^2 \approx \theta_0^2 + \frac{2Q}{k_0}\left(m\frac{k_V}{k_0} - n\right). \quad (40)$$

The resulting diffraction pattern is illustrated by Fig. 2, where incident plane wave with wave vector $\mathbf{k_0}$ as well as all possible wave vectors $\mathbf{k_{n,m}}$ are schematically shown.

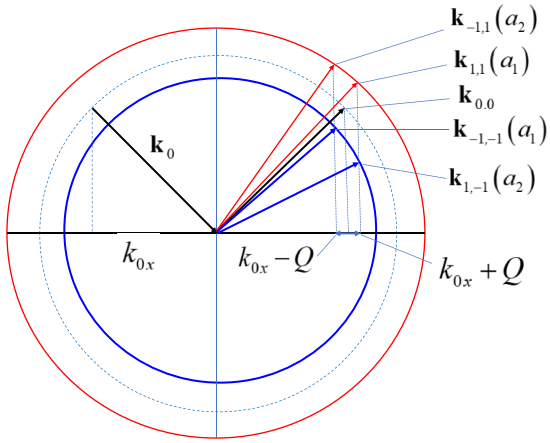

FIG. 2. The outer (red) and inner (blue) circles correspond to neutrons with energies $\omega_1 = \omega_0 + \Omega$ and $\omega_{-1} = \omega_0 - \Omega$, respectively. Here ω_0 is the energy of incoming neutrons. Arrows indicate wave vectors $\mathbf{k}_{n,m}$ of reflected neutrons and x-projections k_{0x} and $k_{0x} \pm Q$ are shown.

The amplitudes of the counterpropagating SAWs $a_{1,2}$, on which the given amplitudes of the reflected waves depend, are shown in parentheses next to them. Figure 2 shows that for $k_V > k_0$, which, as a rule, is true in neutron experiments, the diffraction angles $\theta_{n,m}$ increase in the following order: $\theta_{1,-1}, \theta_{-1,-1}, \theta_{0,0} = \theta_0, \theta_{1,1}, \theta_{-1,1}$.

In the above notation, the wave functions of reflected and transmitted waves are as follows:

$$\Psi_R(x,z,t) = \sum_n \sum_m r_{n,m} \exp(ik_{nx}x - ik_{n,m}z - i\omega_m t), \quad (41a)$$

$$\Psi_T(x,z,t) = \sum_n \sum_m t_{n,m} \exp(ik_{nx}x + iq_{n,m}z - i\omega_m t). \quad (41b)$$

Having written down the wave functions and their derivatives at the interface $z = z_S(x,t)$, and using, as above, the expansion of the exponents of the form $\exp(i\beta \sin\varphi)$ in series Eq. (8) in terms of the Bessel functions, we arrive at a system of equations that determine the wave amplitudes $r_{n,m}$ and $t_{n,m}$. Considering only zero and plus or minus first orders when solving this system, we obtain the following results for the reflection coefficients of the corresponding orders:

$$R_{0,0} = \left|\frac{k_{0z} - q_{0z}}{k_{0z} + q_{0z}}\right|^2, T_{0,0} = \left|\frac{2k_{0z}}{k_{0z} + q_{0z}}\right|^2, \quad (42a)$$

$$R_{n,m} = k_{0z}k_{n,m}a_{n,m}^2 \left|\frac{k_{0z} - q_{0z}}{k_{n,m} + q_{n,m}}\right|^2, (n,m = \pm 1), \quad (42b)$$

where $k_{n,m}$ and $q_{n,m}$ are defined in Eqs. (38), $a_{n,m} = a_1$ for $n = m$ and $a_{n,m} = a_2$ for $n = -m$.

We note here following important circumstance: If $n = m$, then $a_{n,m} = a_1$ and the reflection amplitudes $r_{n,n}$ depend only on the SAW amplitude a_1 and are completely independent of the amplitude a_2 of the counterpropagating wave. The opposite situation takes place for $n = -m$. In other words, each of these reflection amplitudes is absolutely insensitive to the presence or absence of a standing SAW. For appearance of these waves, only the presence of a traveling SAW in a certain direction along the surface is necessary.

The general result is that the solution to the problem of neutron diffraction by a standing acoustic wave is the sum of the solutions for two SAWs traveling in the opposite directions. It seems, however, that the mere fact of representing the equation of the surface of the medium as a superposition of two counterpropagating waves is not enough for the result to be a sum of solutions. The determining factor here is our initial approximation of the smallness of the amplitude of the surface vibration, which allows us to confine ourselves to considering waves of only zero and first orders.

To illustrate this statement, we turn to the expansion Eq. (35) of the incident wave on the oscillating surface Eq. (33). Among the nine terms discussed above, there is, e.g., a term with phase $\phi = (k_{0x} + 2Q)x - \omega_0 t$, describing elastic scattering but with a change in the projection of the wave vector on $2Q$. This term with amplitude $J_1(k_{0z}a_1)J_1(-k_{0z}a_2)$ has an interference nature, though was discarded by us due to the second-order smallness.

The second important circumstance is that the smallness of the SAW amplitudes allowed us to confine ourselves to the kinematic approximation, in which all diffraction orders do not interact with each other and are independent. In the case of a sufficiently "thick" grating, a dynamic approach to the description of diffraction is required, in which the diffraction orders are coupled. Such a case was considered in Ref. [32].

III. NEUTRON DIFFRACTION BY SURFACE WAVES. EXPERIMENT

A. Measurement procedure and raw data treatment

The experiment was performed at the NREX reflectometer of the FRM II reactor (Garching, Germany) [33] with monochromatic (wavelength 4.3 Å with relative wavelength resolution 2%) neutron having angular divergence of 0.04°. A YZ cut of a lithium niobate crystal ($LiNbO_3$) with dimensions 60 x 20 x 3 mm^3 was used as a sample. Two interdigital transducers (IDTs) with an aperture of 5 mm were fabricated by photolithography on the crystal surface. The IDTs allow one to excite a SAW with a wavelength of $\Lambda = 50$ μm and resonant frequency $f = 69.8$ MHz. In the YZ cut of $LiNbO_3$ crystal, a SAW propagates along the polar axis Z with a velocity of $V = 3488$ m/s. During experiment, a high-frequency electrical signal was supplied to one of the two or both IDTs. In the first case, a SAW was excited propagating almost along the neutron beam incident on the sample at a grazing angle ($s = 1$). When voltage was supplied to another IDT, a wave was excited in the opposite direction compared to the first case ($s = -1$). To excite a standing surface wave on the sample surface, a voltage was supplied synchronously to both IDTs. The distance from the IDT to the edges of the sample was 3–4 mm, so the area of the sample occupied by SAW was 53 x 5mm^2. To be sure that we illuminate only the area with the SAW, a cadmium diaphragm with a 5-mm-wide slit was installed at the front end of the sample with respect to the beam. The back end of the sample was covered with a cadmium plate. In the experiment, we used a position-sensitive detector [33] to measure angular distribution of neutron intensity scattered from the sample surface at a set of incident angles θ_0. For every θ_0, the detector was

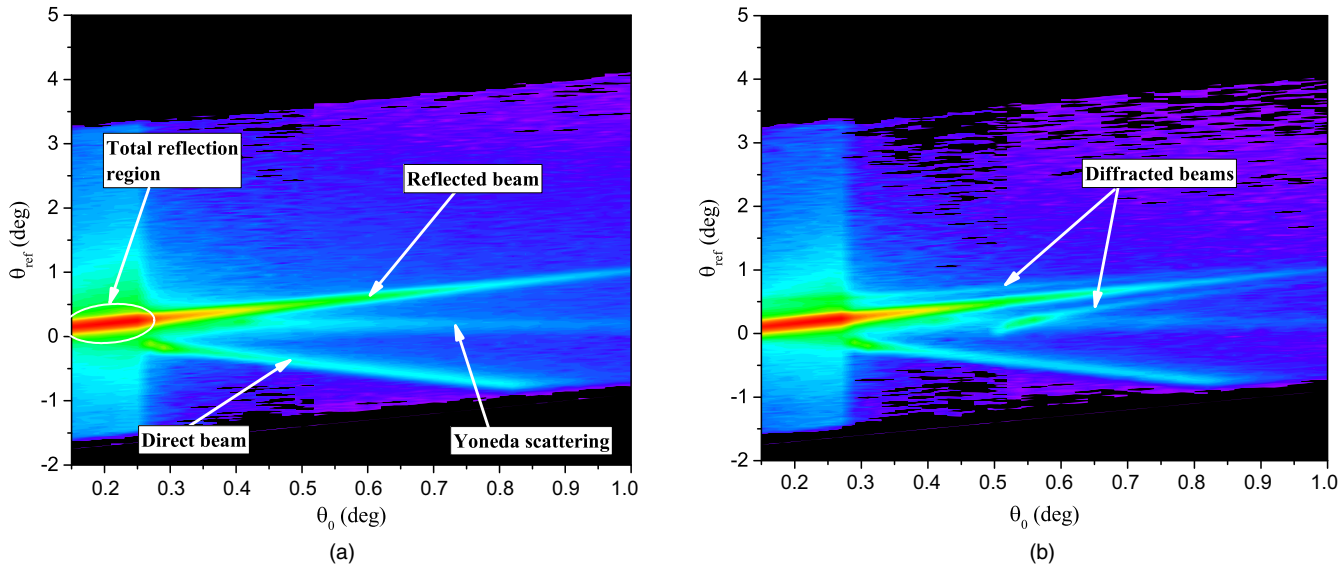

FIG. 3. Two-dimensional scattering map without US wave (a) and with s=-1 wave (b).

set to $2\theta_0$, so the beam corresponding to specular reflection always fell in the same region of the detector (so-called $\theta/2\theta$ geometry). The scattering angles θ_{ref} were then calculated using the sample-detector distance (2500 mm) and distance between two position channels (1 mm) with accuracy of 1.24 arcmin, which later was taken into account in data treatment.

The aim of processing the experimental data was to determine the amplitudes and angles of diffracted waves. The raw data were two-dimensional arrays, the visual representation of which (two-dimensional scattering map) is shown in Fig. 3. Each element of the array contains the number of detector counts corresponding to a certain reflection angle for a given angle of the incident beam. Figure 3(a) presents data obtained in the absence of ultrasonic waves. Three bright bands are clearly visible on it, corresponding to a direct beam partially blocked by a beamstop a specularly reflected beam and a beam caused by off-specular scattering due to the surface roughness with a maximum near the critical angle (Yoneda scattering [34]). In the presence of ultrasonic waves [Fig. 3(b)], this picture is supplemented by two bands, which are due to neutron diffraction by the SAW. All reflected beams are characterized by some, generally speaking, asymmetric, angular distribution. As for the specularly reflected beam, its angular distribution is determined by the conditions of formation of the incident beam, including the design of the crystal monochromator, the geometry and physical features of the forming slits, and so on. Upon reflection, an additional distortion of the beam shape arises due to the nonideal flatness of the sample. Apparently, the only way to find the angular distance between the specular and diffracted beams is to calculate the difference between the positions of the model functions that describe well the physical angular distribution of the beams. In this case, one has to make an assumption that the shape of all the beams is completely identical. This assumption is not only natural, but, apparently, the only possible one, since otherwise the concept of the angular distance between extended and asymmetric beams is uncertain. Moreover, the only requirement for these fitting functions is a good description of the initial angular distributions. There is probably a sufficiently large variety of such model functions, the choice between which is to some extent arbitrary. The specific form of these functions should not be given any physical meaning.

To analyze data without a SAW, a fitting function of the following form was used:

$$\begin{aligned} f_0(x, x_{0J}, A_J, \sigma_J, \mu) = y_0 &+ F_D(A_D, x, x_{0D}, \sigma_{1D}, \sigma_{2D}) \\ &+ F_R(A_R, x, x_{0R}, \mu, \sigma_{1R}, \sigma_{2R}) \\ &+ F_Y(A_Y, x, x_{0Y}, \sigma_Y), \end{aligned} \tag{43}$$

where

$$F_D(A_D, x, x_{0D}, \sigma_{1D}, \sigma_{2D}) = \begin{cases} A_D \exp\left[-\frac{(x-x_{0D})^2}{2\sigma_{1D}^2}\right], & x \leqslant x_{0D} \\ A_D \exp\left[-\frac{(x-x_{0D})^2}{2\sigma_{2D}^2}\right], & x > x_{0D}, \end{cases} \tag{44a}$$

$$\begin{aligned} F_R(A_R, x, x_{0R}, \sigma_{1R}, \sigma_{2R}) &= \mu A_R \left(\frac{2}{\pi}\right) \frac{\sigma_{1R}}{(x-x_{0R})^2 + \sigma_{1R}^2} \\ &+ (1-\mu) A_R \exp\left[-\frac{(x-x_{0R})^2}{2\sigma_{2R}^2}\right], \end{aligned} \tag{44b}$$

$$F_Y(A_Y, x, x_{0Y}, \sigma_Y) = A_Y \left(\frac{2}{\pi}\right) \frac{\sigma_Y}{(x-x_{0Y})^2 + \sigma_Y^2}. \tag{44c}$$

Here symbols $J = D, R, Y$ stand for direct (D), reflected (R) beams, and Yoneda (Y) peak; x_{0J} is the positions of a peak with an amplitude A_J and width σ_{1J}, σ_{2J}, and σ_Y, μ is the weight coefficient of the mixed Gauss-Lorentz distribution.

When analyzing the data obtained in the presence of a traveling SAW, the fitting function was supplemented by two terms $F_{\pm 1}$ corresponding to diffracted waves of the ± 1 order. The shape of the latter was assumed to be identical to the

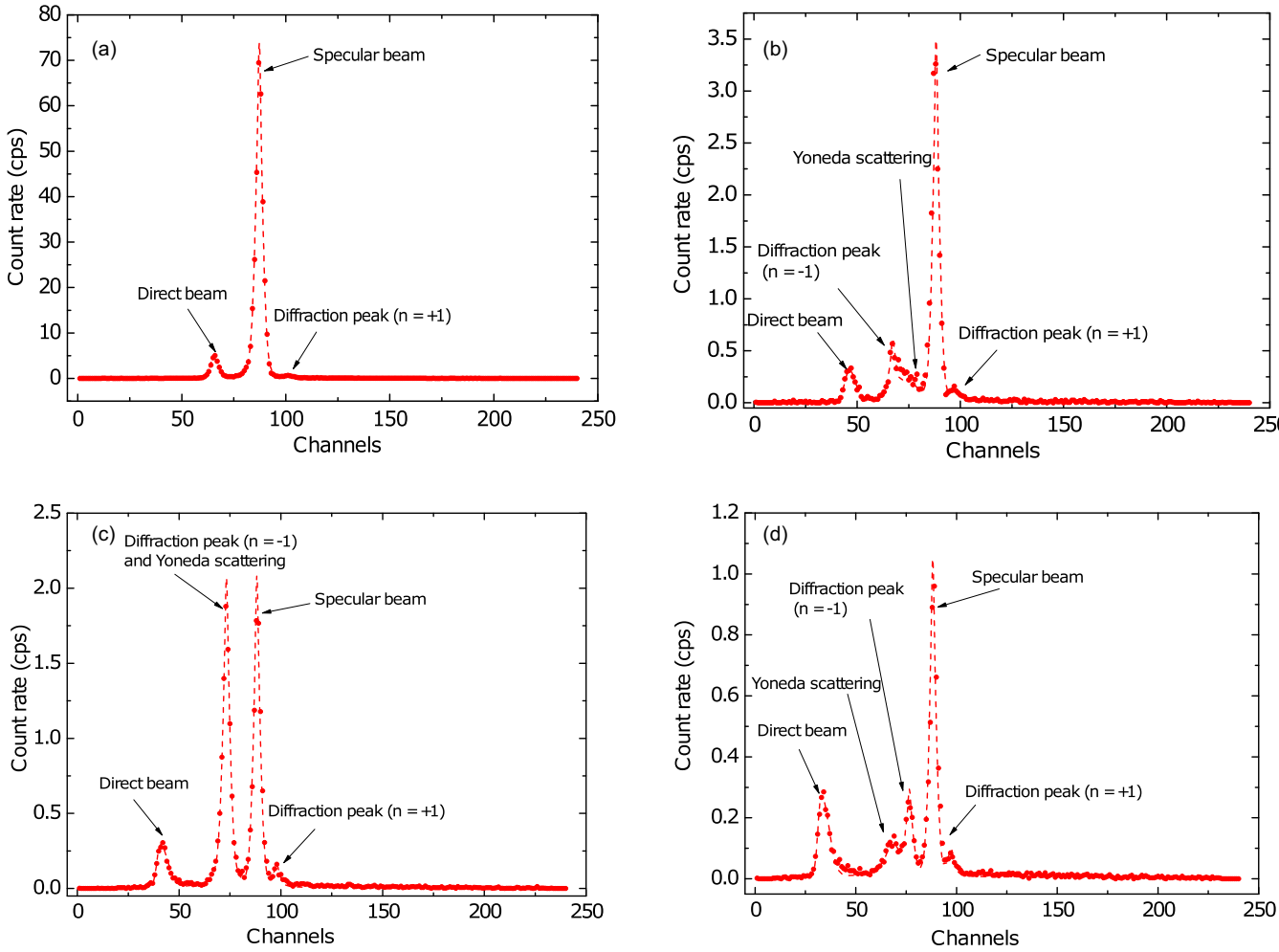

FIG. 4. Intensity as a function of reflection angle for incidence angles of 0.31(a), 0.51(b), 0.56(c) and 0.64(d) degrees. Dashed curves are approximating functions (44), points are experiment.

shape of the peak of the specularly reflected beam:

$$\begin{aligned} f_{AW}(x, x_{0J}, A_J, \sigma_J, \mu) = y_0 &+ F_D(A_D, x, x_{0D}, \sigma_{1D}, \sigma_{2D}) \\ &+ F_R(A_R, x, x_{0R}, \mu, \sigma_{1R}, \sigma_{2R}) \\ &+ F_Y(A_Y, x, x_{0Y}, \sigma_Y) \\ &+ F_{+1}(A_{+1}, x, x_{0,+1}, \mu, \sigma_{1R}, \sigma_{2R}) \\ &+ F_{-1}(A_{-1}, x, x_{0,-1}, \mu, \sigma_{1R}, \sigma_{2R}). \end{aligned} \tag{45}$$

In this case, the free parameters were the amplitudes of the specular and diffracted beams and their positions $x_{0,\pm1}$. In the case of a standing wave, there were three such functions (see below).

For each of the three experiments, with a SAW running in two directions, and with a standing wave, the treatment procedure was repeated again. A complete measurement cycle with waves traveling in two directions and with a standing wave was carried out twice with slightly different amplitudes of the US wave. The results obtained in these measurements are very similar and the demonstration material below refers to only one of these series. Examples of the obtained dependencies of the counting rate on the channel number for the case when the US wave propagated toward the neutron beam ($s = -1$) are shown in Fig. 4.

B. Diffraction angles

The experimental data obtained as a result of the analysis procedure described above were compared with the results of calculations by formula Eq. (32). In the figures below, the calculation results are shown by solid lines. Figure 5 shows the results obtained in the traveling SAW mode.

In the case of excitation of a standing SAW, four beams were recorded in both measurements, including a specular beam. However, the beam with $n = +1$, $m = +1$ was not detected during the experiment. The position of the remaining three beams is in satisfactory agreement with calculation Eq. (40) (see Fig. 6).

It can be seen that the positions of the diffraction peaks are in a good agreement with the calculated values, and the diffraction pattern arising from neutron diffraction by standing waves generally corresponds to the concept of additivity of the diffraction pattern for two SAWs traveling in opposite directions. An unexpected result consists of the appearance of the so-called "anomalous" wave corresponding to the opposite direction of propagation of the ultrasonic wave [lower curve

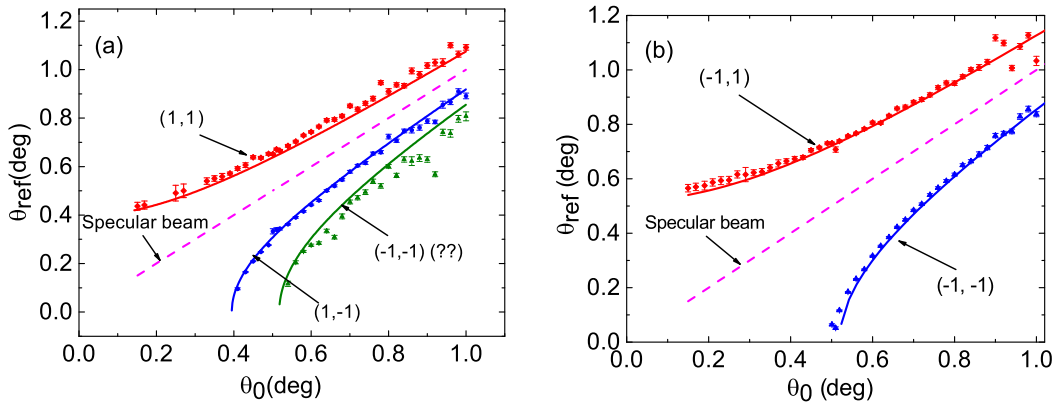

FIG. 5. Angular distributions of diffracted beams depending on the incident angle for the $s = +1$ (a) and $s = -1$ (b) case. Fit and experiments are shown by solid lines and dots. The index s of the direction of propagation of the SAW and order of reflection n are shown in parentheses in form (s, n).

in Fig. 5(a)]. With regard to the absence of the beam with $n = +1$, $m = +1$ during diffraction on a standing wave (Fig. 6), it seems that it was not detected by the applied processing procedure (see the discussion in Sec. III D below).

C. Intensity of diffracted waves

Since a SAW amplitude a was not measured at the experiment, we fitted this parameter to the experimental data. The calculations were carried out in the first order of smallness of the parameter $k_{0z}a$, where k_{0z} is the normal component of the wave vector of incident neutrons. The intensity of the specularly reflected beam (zero-order wave) was used as a monitor; therefore, all experimental and theoretical results were presented as the ratio of the intensity of the wave of the corresponding order to the intensity of the specular beam $I_{\pm1}(k_{0z}) = R_{\pm1}(k_{0z})/R_0(k_{0z})$ [see expressions Eqs. (31)]. As a result of the fit, we obtained $a = 21$ Å ($s = +1$), $a = 22$ Å ($s = -1$) for the traveling SAW (Fig. 7) and $a = 13$ Å for the case of standing SAW (Fig. 8).

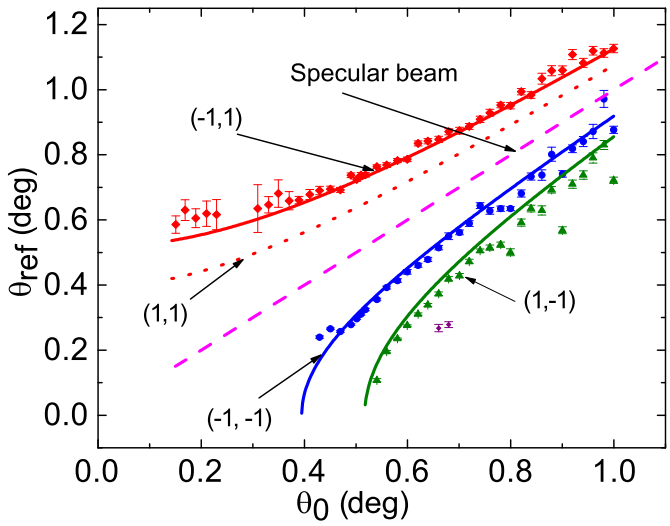

FIG. 6. Angular distributions of diffracted beams depending on the incident angle for the case of standing SAW. Fit and experimental data are shown by solid lines and dots. The order of reflection n and index m are shown in parentheses in form (n, m).

As it follows from Fig. 7, these amplitudes allow for satisfactory agreement of data with the calculation for the case of "normal" waves. As for the "anomalous" wave, conventionally indicated in Fig. 6 as $(1, -1)$, then we will address the question of its amplitude below (see Sec. III D).

In the measurements with a traveling wave (Fig. 7), the dependence of the intensity on the incident angle for "normal" waves was in satisfactory agreement with the calculation. Similar agreement was obtained also for the case of standing wave (Fig. 8), though some discrepancy was observed in the behavior of the "tails" of minus one order for high incidence angle. In this case, two moments should be taken into account. First, in the conditions of traveling and standing waves, the intensities of the corresponding orders differed about three times, which made it difficult to analyze the picture with standing waves. Second, as can be seen in Fig. 6, with an increase in the incident angle, not only does the absolute intensity of the wave of the corresponding order decrease, but also the angular distance between adjacent beams decreases, which also increases the analysis error.

D. Discussion of experimental results

The main experimental results can be summarized as follows:

(1) The angular position of the beams of all diffraction orders is in satisfactory agreement with the theory.

(2) The dependence of the intensity of diffracted waves on the incidence angle is in good agreement with the calculation performed up to the first order of the parameter $k_{0z}a$. Absolute intensity values could not be compared with the calculation due to the lack of data on the amplitude of the SAW.

(3) The experiment confirms the validity of the concept of a standing SAW as a superposition of two traveling SAWs.

(4) Two circumstances distinguish experimental results from theoretical expectations. This is the absence of a single diffraction order (1,1) in measurements with a standing wave (Fig. 6) and the appearance of an "anomalous" diffracted wave in measurements with a SAW propagating along the neutron beam [Fig. 5(a)].

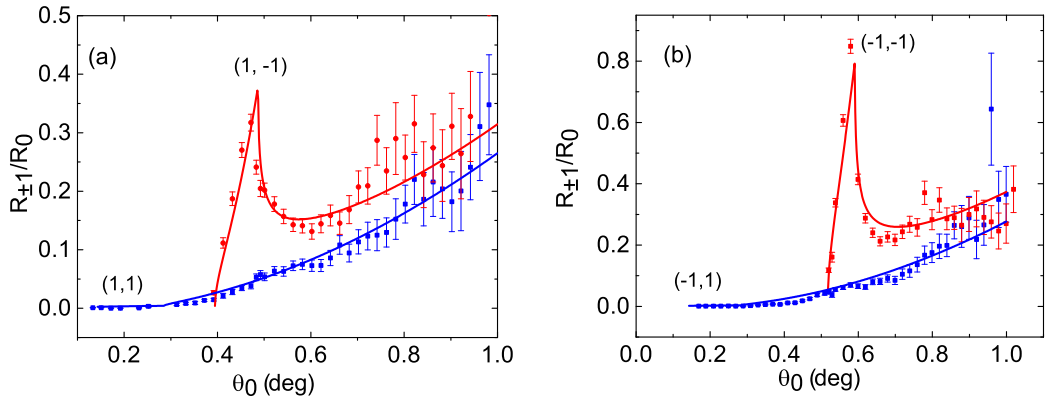

FIG. 7. Amplitudes of diffracted beams as a function of incident angle for the case of traveling wave of $s = +1$ (a) and $s = -1$ (b). Fit and experimental data are shown by solid lines and dots. The index s of the direction of propagation of the SAW and order of reflection n are shown in parentheses in the form (s, n).

First, we recall that all measurements were performed twice, and there were no visible differences in the results of these two measurements. Thus, both the absence of the (+1,+1)-order wave in measurements with a standing wave and the appearance of an "anomalous wave" that is absent in measurements without a SAW cannot be regarded as an accident. However, these two facts should be treated differently.

The fact is that the absolute intensity of the diffraction orders is rather small, therefore, the conditions for separating the diffraction beam from the full two-dimensional pattern are quite difficult. This is illustrated in particular by Fig. 3. It clearly shows that small peaks of diffraction orders are often located on the wings of much more intense beams. Figure 9 illustrates the difficulty of detecting diffraction orders (1,1) and (−1,1). It shows absolute values of the reflectivities of these waves together with the specular reflectivity. One can see that the angular position of the maximums with $n = +1$ practically coincides with the critical angle of the total external reflection. Under these conditions, the background of nonspecular reflection due to scattering on surface roughness is relatively large. This makes it extremely difficult to isolate diffracted beams with amplitudes three orders of magnitude smaller than the specular reflectivity. This is especially true for the beam (1,1) absent in data treatment, which, as can be seen in Fig. 6, is located closer to the direct beam than the detected beam (−1,1). As for the beams (−1,−1) and (1,−1), the maximum of their intensity lies at relatively large incident angles, where the intensity of the direct beam is significantly weakened. Accordingly, the background conditions for their registration are much better than for the beams with $m = +1$.

As for the observation of an "anomalous" wave, presence of which was not predicted, the situation here is substantially different, and an explanation should be sought for this fact. In the case under consideration, the origin of the anomaly can be associated either with the appearance of a wave of the second diffraction order ($s = +1, n = -2$), or with the presence of a wave traveling in the opposite direction compared to the main wave, i.e., from $s = -1, n = -1$. The calculated angular position of these two waves is very close and it is impossible to draw a definite conclusion based on the analysis of the angular picture. However, the relatively high intensity of this wave, amounting to approximately 0.3 of the intensity of the "normal" wave $s = +1, n = -1$, allows one to confidently reject the hypothesis of a second-order wave, the intensity of which should be tens of times lower.

Thus, the most probable reason for the appearance of this beam is the presence of a counterpropagating wave ($s = -1$) on the surface of the sample. The appearance of such a wave

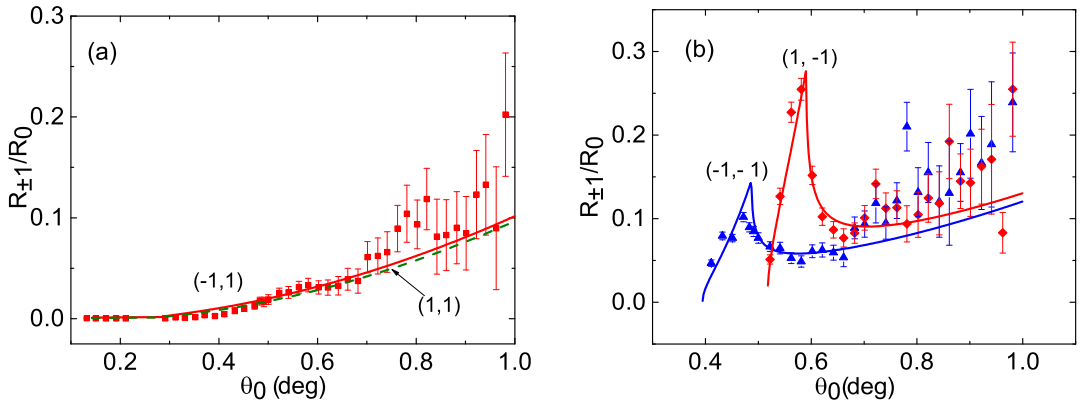

FIG. 8. Amplitudes of diffracted beams as a function of incident angle for the case of standing SAW. Fit and experimental data are shown by solid lines and dots. The order of reflection n and index m are shown in parentheses in the form (n, m).

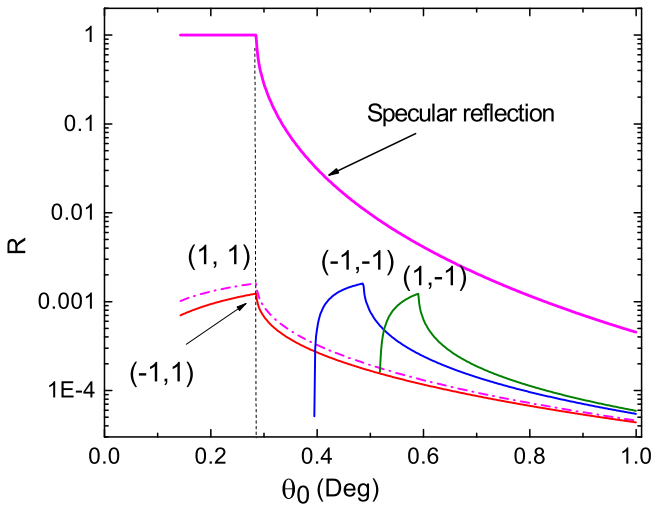

FIG. 9. Calculated "reflectivities" R for the case of four diffracted waves in the standing SAW geometry for the amplitude of SAW 13 Å in comparison with specular reflectivity.

can be due to both the unclosed initial portion of the sample between the IDT and the sample edge, and the reflection of the SAW from the trailing edge of the sample or from the second (free) IDT.

However, we note that, having accepted this hypothesis, we are faced with the need to answer the question about the reason for the absence of an "anomalous" longitudinal surface wave ($s = 1$) in measurements in the geometry of the counterpropagating wave. There is no definite answer to this question, and we can only appeal to the above considerations about the difficulty of detecting weak beams near an intense specular reflection beam.

IV. CONCLUSION

This paper presents results of a theoretical and experimental study of nonstationary neutron diffraction by SAWs. For traveling and standing waves, the solution of the diffraction problem was found by a unified method based on the expansion of waves in spatial and frequency harmonics, followed by matching at the interface of the wave functions of the incident, diffracted, and transmitted waves. The found systems of equations completely determine the solution to the problem. In a practically realizable approximation of the smallness of parameter $\xi = k_{0z}a$ (k_{0z} is the normal component of the wave vector of the incident wave, a is the amplitude of the surface waves) the solution can be found analytically. It is shown that the diffraction pattern by standing waves found in this approximation can be represented as a result of diffraction by two counterpropagating and completely independent traveling surface waves. Expressions are given that describe both the angular distribution and the amplitudes of the corresponding diffracted waves. The results related to the case of a traveling wave coincide with those given earlier in Ref. [19], where the solution was obtained in a moving rest frame of the surface structure.

Diffraction spectra were measured using a neutron reflectometer with a fixed neutron wavelength of 0.43 nm and a variable incident angle. The experiment showed that the position of the waves of all diffraction orders and the dependence of the intensity of the diffracted waves on the incidence angle are in good agreement with the calculation performed up to the first order of the parameter $k_{0z}a$. The absolute values of the intensity could not be compared with the calculation due to the lack of data on the amplitude of the SAW.

The results obtained for diffraction by a standing wave are in complete agreement with the concept of it as a superposition of two traveling waves.

Two circumstances distinguish experimental results from theoretical expectations. This is the absence of a single diffraction order in measurements with a standing wave and the appearance of an anomalous wave in measurements with a wave traveling along the neutron beam. Possible sources of these discrepancies in the work are discussed, but the final answer about the methodological or fundamental origin of these anomalies can be obtained only in subsequent experiments.

ACKNOWLEDGMENTS

This work is based on experiments performed at the NREX instrument operated by the Max Planck Society at the MLZ (Garching, Germany). Y.N.K. would like to thank Thomas Keller for fruitful discussions and the Deutsche Forschungsgemeinschaft (DFG, German Research Foundation) for financial support (Project No. 107745057—TRR 80).

[1] P. Debye and F. W. Sears, Proc. Nat. Acad. Sci. U.S.A. **18**, 409 (1932).
[2] R. Lucas and P. Biquard, J. Phys. Radium **3**, 464 (1932).
[3] C. V. Raman and N. S. Nagendra Nath, Proc. Indian Acad. Sci. **A2**, 406 (1935); **A2**, 413 (1935); **A3**, 75 (1936); **A3**, 119 (1936); **A3**, 459 (1936).
[4] V. I. Balakshy, V. N. Parygin, and L. E. Chirkov, *Physical Basis of Acousto-optics (in Russian)* (Radio i svyaz', Moscow, 1985).
[5] A. Korpel, *Acousto-optics*, Vol. 57 (CRC Press, Boca Raton, 1996).
[6] S. Kikuta, T. Takahashi, and S. Nakatani, Jpn. J. Appl. Phys. **23**, L193 (1984).
[7] H. Cerva and W. Graeff, Phys. Status Solidi A **82**, 35 (1984).
[8] I. R. Entin, Phys. Status Solidi B **132**, 355 (1985).
[9] A. Erko, A. Firsov, D. Roshchoupkin, and I. Schelokov, in *Modern Developments in X-ray and Neutron Optics* (Springer, Berlin, 2008), pp. 471–500.
[10] T. F. Parkinson and M. W. Moyer, Nature **211**, 400 (1966).
[11] A. G. Klein, P. Prager, H. Wagenfeld, P. J. Ellis, and T. M. Sabine, Appl. Phys. Lett. **10**, 293 (1967).
[12] B. Chalupa, R. Michalec, V. Petržílka, J. Tichý, and J. Zelenka, Phys. Status Solidi B **29**, K51 (1968).
[13] R. Michalec, B. Chalupa, J. Čech, V. Petržílka, S. Kadečková, and O. Taraba, Phys. Lett. A **29**, 679 (1969).
[14] E. Raitman, V. Gavrilov, and Ju. Ekmanis, in *Modeling and Measurement Methods for Acoustic Waves and for Acoustic*

Microdevices, edited by M. G. Beghi (IntechOpen, Rijeka, 2013), Chap. 3.
[15] T. Takahashi, E. Granzer, H. Tomimitsu, S. Kikuta, and K. Doi, Jpn. J. Appl. Phys. **24**, 218 (1985).
[16] T. Takahashi, E. Granzer, H. Tomimitsu, S. Kikuta, and K. Doi, Jpn. J. Appl. Phys. **24**, L650 (1985).
[17] W. A. Hamilton and M. Yethiraj, Phys. Rev. B **59**, 3388 (1999).
[18] I. M. Frank, Possible cause of anomaly in storage time of ultracold neutrons, JINR communications (JINR, Dubna, 1975) P4-8851 (in Russian).
[19] W. A. Hamilton, A. G. Klein, G. I. Opat, and P. A. Timmins, Phys. Rev. Lett. **58**, 2770 (1987).
[20] D. T. W. Toolan, R. Barker, T. Gough, P. D. Topham, J. R. Howse, and A. Glidle, J. Colloid Interface Sci. **487**, 465 (2017).
[21] Yu. N. Pokotilovski, Phys. Lett. A **255**, 173 (1999).
[22] S. K. Lamoreaux and R. Golub, Phys. Rev. C **66**, 044309 (2002).
[23] A. I. Frank and V. G. Nosov, Phys. Lett. A **188**, 120 (1994).
[24] A. I. Frank, S. N. Balashov, I. V. Bondarenko, P. Geltenbort, P. Høghøj, S. V. Masalovich, and V. G. Nosov, Phys. Lett. A **311**, 6 (2003).
[25] A. I. Frank, P. Geltenbort, G. V. Kulin, D. V. Kustov, V. G. Nosov, and A. N. Strepetov, JETP Lett. **81**, 427 (2005).
[26] J. Felber, R. Gähler, C. Rausch, and R. Golub, Phys. Rev. A **53**, 319 (1996).
[27] A. I. Frank, JETP Lett. **100**, 613 (2015).
[28] A. I. Frank, D. V. Kustov, G. V. Kulin, S. V. Goryunov, D. V. Roshchupkin, and D. V. Irzhak, J. Phys.: Conf. Ser. **746**, 012054 (2016).
[29] V. F. Sears, *Neutron Optics: An Introduction to the Theory of Neutron Optical Phenomena and their Applications*, Oxford series on neutron scattering in condensed matter (Oxford University Press, New York, 1989).
[30] I. M. Frank, Phys. Usp. **34**, 988 (1991).
[31] L. Li, J. Chandezon, G. Granet, and J.-P. Plumey, Appl. Opt. **38**, 304 (1999).
[32] V. A. Bushuev, A. I. Frank, and G. V. Kulin, JETP **122**, 32 (2016).
[33] Yu. Khaydukov, O. Soltwedel, and T. Keller, JLSRF **1**, A38 (2015).
[34] Y. Yoneda, Phys. Rev. **131**, 2010 (1963).